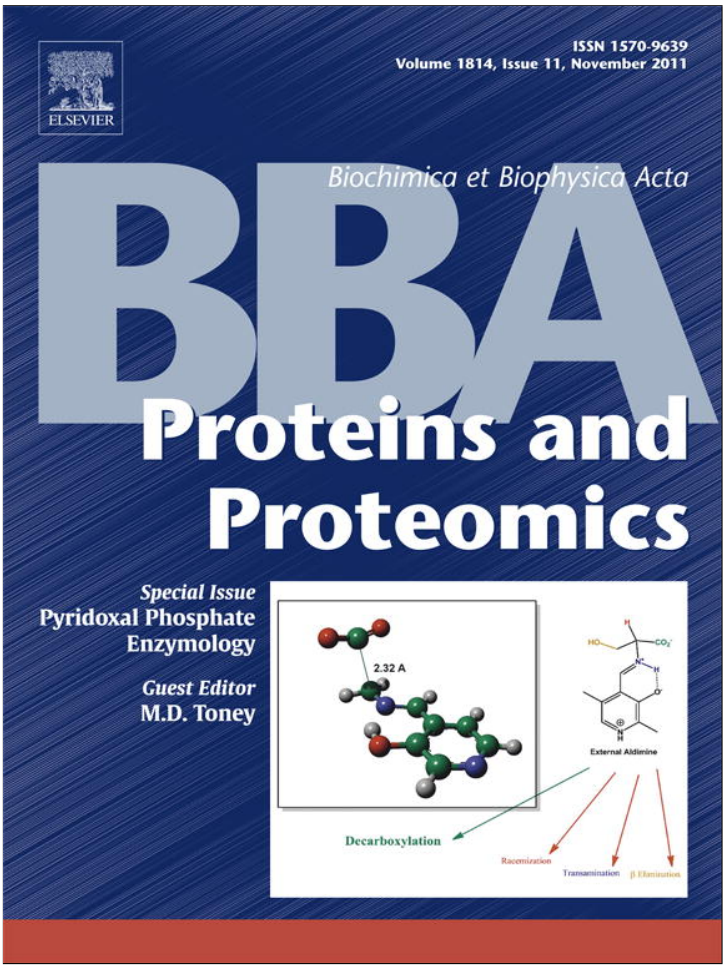

Biochimica et Biophysica Acta 1814 (2011) 1426–1437

Contents lists available at ScienceDirect

Biochimica et Biophysica Acta

journal homepage: www.elsevier.com/locate/bbapap

Review

Critical hydrogen bonds and protonation states of pyridoxal 5′-phosphate revealed by NMR☆

Hans-Heinrich Limbach [a,*], Monique Chan-Huot [a], Shasad Sharif [a], Peter M. Tolstoy [a], Ilya G. Shenderovich [a], Gleb S. Denisov [b], Michael D. Toney [c]

[a] Institut für Chemie und Biochemie, Freie Universität Berlin, Takustraβe 3, D-14195 , Germany
[b] Institute of Physics, St. Petersburg State University, 198504 St. Petersburg, Russian Federation
[c] Department of Chemistry, University of California-Davis, 95616 Davis, USA

ARTICLE INFO

Article history:
Received 31 March 2011
Received in revised form 4 June 2011
Accepted 7 June 2011
Available online 16 June 2011

Keywords:
Pyridoxal 5′-phosphate
Aspartate aminotransferase
Tautomerism
Protonation state
Hydrogen bonding
Solid and liquid state NMR

ABSTRACT

In this contribution we review recent NMR studies of protonation and hydrogen bond states of pyridoxal 5′-phosphate (PLP) and PLP model Schiff bases in different environments, starting from aqueous solution, the organic solid state to polar organic solution and finally to enzyme environments. We have established hydrogen bond correlations that allow one to estimate hydrogen bond geometries from ^{15}N chemical shifts. It is shown that protonation of the pyridine ring of PLP in aspartate aminotransferase (AspAT) is achieved by (i) an intermolecular OHN hydrogen bond with an aspartate residue, assisted by the imidazole group of a histidine side chain and (ii) a local polarity as found for related model systems in a polar organic solvent exhibiting a dielectric constant of about 30. Model studies indicate that protonation of the pyridine ring of PLP leads to a dominance of the ketoenamine form, where the intramolecular OHN hydrogen bond of PLP exhibits a zwitterionic state. Thus, the PLP moiety in AspAT carries a net positive charge considered as a pre-requisite to initiate the enzyme reaction. However, it is shown that the ketoenamine form dominates in the absence of ring protonation when PLP is solvated by polar groups such as water. Finally, the differences between acid–base interactions in aqueous solution and in the interior of proteins are discussed. This article is part of a special issue entitled: Pyridoxal Phosphate Enzymology.

1. Introduction

Pyridoxal 5′-phosphate (PLP, Scheme 1) is a cofactor of enzymes that are responsible for amino acids transformations such as racemization, transamination and decarboxylation [1–4] among others. PLP contains four functional groups, and therefore, a number of different chemical, protonation, hydrogen bond and tautomeric states whose facile interconversion is a pre-requisite for its catalytic activity. In water it is present under the form of an aldehyde (Scheme 1a) or of an hydrate (Scheme 1b). With amino groups it forms Schiff bases, called "aldimines" if the reaction takes place with saturated amines or amino acids, and "aldenamines" in the case of unsaturated amines (Scheme 1c). When PLP is embedded in an enzyme it usually forms the so-called "internal aldimine" with the ε-group of a lysine residue in the active site, or "external aldimines" with amino acid substrates or inhibitors. Finally, it may also form a geminal diamine as an intermediate in the interconversion of aldimines or in condensation with polyamines (Scheme 1d).

The first step of all PLP dependent enzyme reactions is the replacement of the lysine residue with the amino group of an incoming amino acid substrate producing an external aldimine. This reaction is called "transimination"[5]. It has been argued that the nucleophilic attack in the first step of the latter reaction requires a positive charge on the Schiff base imino nitrogen [1,6–8]. For that, the bridging proton of the intramolecular OHN hydrogen bond has to be transferred from the phenolic oxygen to the imino nitrogen. This reversible proton tautomerism may be assisted by protonation of the pyridine ring (Scheme 2).

Some of us have used liquid and solid state NMR techniques to study proton transfer and hydrogen bonding in the past decades [9,10]. Therefore, we have applied these techniques to the study of the protonation, hydrogen bond and tautomeric states of PLP species in various environments. Protonation states in aqueous solution were studied in the case of PLP [11,12] and of model PLP Schiff bases [13]. The latter were also studied by X-ray crystallography [14] and NMR in the solid state [15], by liquid state NMR in polar solution [16,17] and, finally, in an enzymatic environment, *i.e.* aspartate aminotransferase (AspAT) [18].

In this review, we will address the following questions. What is the nature of the two OHN hydrogen bonds of PLP Schiff bases? Is there a coupling between both hydrogen bonds? How are these bonds influenced by the environment? Is there a difference between the

☆ This article is part of a special issue entitled: "Pyridoxal Phosphate Enzymology".

* Corresponding author. Tel.: +49 3083855375; fax: +49 3083855310.
E-mail address: limbach@chemie.fu-berlin.de (H.-H. Limbach).

1570-9639/$ – see front matter © 2011 Published by Elsevier B.V.
doi:10.1016/j.bbapap.2011.06.004

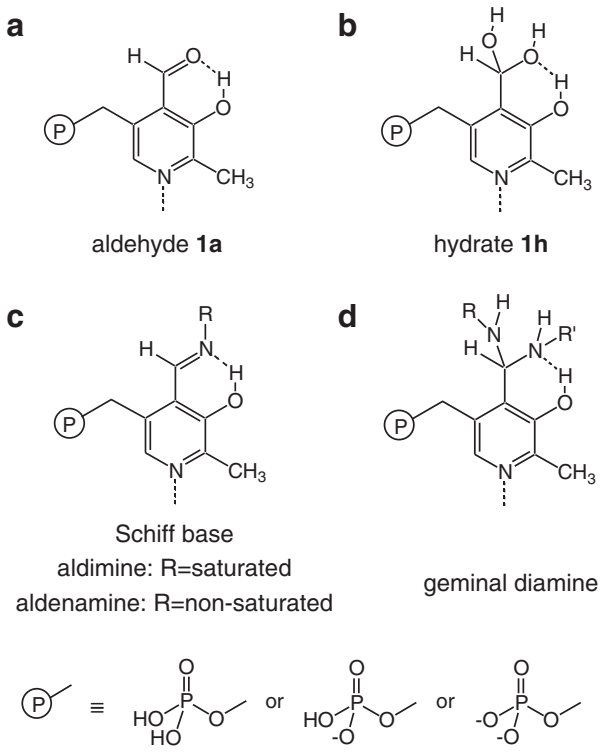

Scheme 1. Main chemical structures of pyridoxal 5′-phosphate (PLP). (a) Aldehyde 1a, (b) hydrate 1h, (c) Schiff base, (d) geminal diamine.

organic solid state, organic polar liquid state, water and the enzyme environment? What kind of environment is realized in the latter?

In order to facilitate the discussion, we will initially discuss the protonation states of PLP and PLP model Schiff bases in aqueous solution. Then, we will describe their properties in the organic solid state and polar solution, and finally, the properties of PLP as internal aldimine in AspAT.

2. Chemical states and protonation states of PLP in aqueous solution

The protonation states of PLP in water have been explored recently using a combination of ^{15}N NMR of PLP labeled with ^{15}N in the pyridine ring (1-^{15}N) [11] and ^{13}C NMR of (1-$^{13}C_2$) [12]. The structures of the labeled compounds as well as the resulting protonation pattern are illustrated in Scheme 3. The protonation states are labeled by Roman numerals which indicate the number of protons removed from the fully protonated compound. These protonation states refer to the whole molecule, and not necessarily to a given acid–base center. The consequence is a proton tautomerism of protonation states I, II and III as depicted in Scheme 3. In order to specify the tautomers, it is useful to label the three acid–base centers of PLP. Thus, we label the phosphate group as AH_2, AH or A, the pyridine ring as BH or B, and the phenol group as XH or X, where electrical charges are omitted. A given protonation and tautomeric state can then be characterized by a combination of the labels of the three acid–base centers.

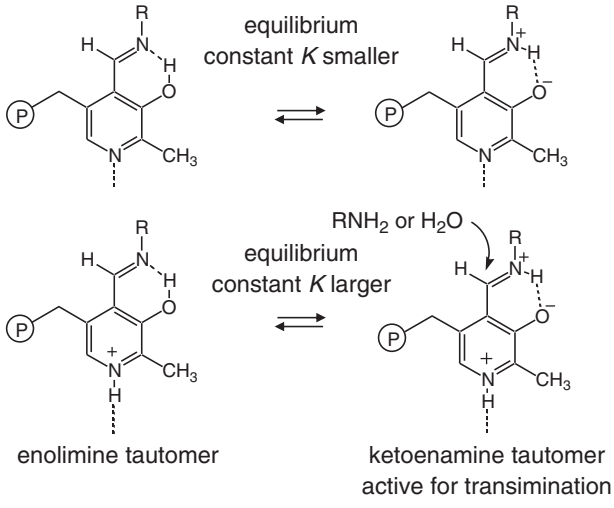

Scheme 2. Tautomerism of PLP Schiff bases between an enolimine and a ketoenamine form depending on the protonation of the pyridine ring. Adapted from Ref. [17].

In order to observe an effect of pH on the NMR signal of a given nucleus its chemical shift must change upon protonation/deprotonation. As proton transfer is fast in the NMR time scale, only signals are observed which represent averages over all protonation and tautomeric states. The chemical shift of the methylene carbon shows little dependence on the pH. By contrast, the ^{13}C nucleus in the aldehyde or hydrate site is of diagnostic value. Thus, by analysis of the pH dependence of the signal of this carbon all four pK_a values linking protonation states 0 to IV could be obtained both for the aldehyde, dominating at high pH, and for the hydrated form, dominating at low pH [12]. The pK_a values of both species are not very different; the largest difference occurs for the interconversion between protonation states I and II.

On the other hand, ^{13}C NMR exhibits little diagnostic value for the tautomeric processes, in contrast to ^{15}N NMR [11]. The chemical shift of the pyridine ^{15}N nucleus changes strongly if the pyridine N is protonated or deprotonated. The average signal position then depends on the equilibrium constant of tautomerism. In protonation state 0 only BH is formed and in IV only B providing the intrinsic limiting chemical shifts at low and at high pH. In the hydrate, the pyridine is protonated almost entirely in all protonation states besides IV. By contrast, in protonation states II and III of the aldehyde the proton is almost equally located on the pyridine N or the phenolic oxygen. In protonation state I of the aldehyde, the proton is located entirely on the pyridine ring and not on the phosphate.

In summary, one cannot associate independent pK_a values to the acid–base centers of PLP as they depend on each other. The location of a proton in a given overall molecular protonation state depends on the equilibrium constant of tautomerism, which – for a given protonation state – is independent of pH. The pK_a values of the aldehyde and of the hydrate are not very different, but the equilibrium constants of tautomerism are. Thus, the pyridine N of the hydrate is entirely protonated below pH 8.7, but only to about one half in the aldehyde below pH 8.3. Full protonation only occurs below pH 3.6.

3. Chemical states and protonation states of PLP in the presence of amines and L-lysine in aqueous solution

In the past, PLP Schiff bases have been mainly studied by UV–Vis absorption techniques [19–22]. However, UV–Vis spectroscopy lacks the chemical selectivity provided by multinuclear NMR spectroscopy. Therefore, ^{1}H or ^{13}C NMR at natural abundance in combination with UV–Vis absorption techniques has been applied [19–21]. Recently, a combination of ^{13}C and ^{15}N NMR has been used to obtain detailed information about the protonation states and the intramolecular tautomerism of PLP aldimines [13].

In Scheme 4 depicted are the protonation states of different reaction products of PLP with amino groups. For simplification we use abbreviated structures which highlight the functional groups. Scheme 4a depicts the case of an external or internal aldimine exhibiting five protonation states as PLP itself. The model aldimine of Scheme 4b formed by PLP with a diamine exhibits an additional protonation state arising from the free amino group. Six protonation

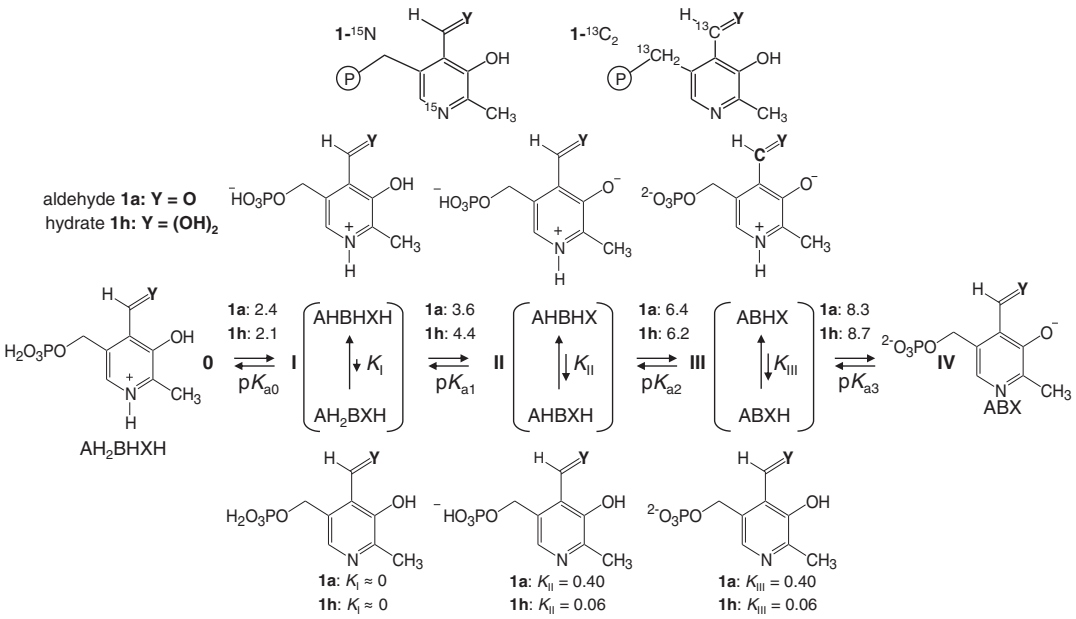

Scheme 3. Protonation states of PLP in aqueous solution. Adapted from Refs. [13] and [17].

states are also conceivable for a geminal diamine, for example the cyclic geminal diamine of Scheme 4c. For simplification, we depict in Scheme 4 only the ketoenamine tautomer, but the question arises of how much the enolimine tautomer is formed in each protonation state. As the pK_a values and equilibrium constants of tautomerism of the species in Scheme 4 depend on the chemical structure, we will only discuss two representative cases in the following.

The simplest model of an internal aldimine is the methyl Schiff base 2 of PLP which was either labeled with ^{15}N in the ring or in the imino position. This species is stable in water only above pH 5; below that it decomposes into PLP and the protonated amine. The ^{15}N chemical shifts of 2 measured recently [11] are plotted in Fig. 1 as a function of pH. The pyridine N of 2 is protonated at low and deprotonated at high pH, exhibiting a pK_a value of 5.8. There is no apparent proton tautomerism between the pyridine N and the phenolic oxygen, in contrast to PLP. The protonation states of the phosphate group do not influence the ^{15}N chemical shifts within the margin of error. In analogy to PLP, from pH 6 and above the doubly deprotonated phosphate group dominates. The imino nitrogen of 2 is protonated up to pH 11.4. The high pK_a value is partially due to the negative charge of the phosphate group; if the latter is removed, the pK_a value drops to 10.5 as demonstrated for the case of 3. No sign of proton tautomerism according to Scheme 2 is observed. Thus, either the ketoenamine tautomer is formed entirely exhibiting still the intramolecular hydrogen bond, or the latter is broken by hydrogen bonding to water molecules [11]. We note that a recent computational study by Lin and Gao [23] showed that the enolimine tautomer is not favored in water in the methyl N-substituted Schiff base, but it becomes stabilized – depending on the protonation state of the pyridine ring – when a carboxylate group is introduced. This stabilization plays an important role in the following enzyme reaction [24].

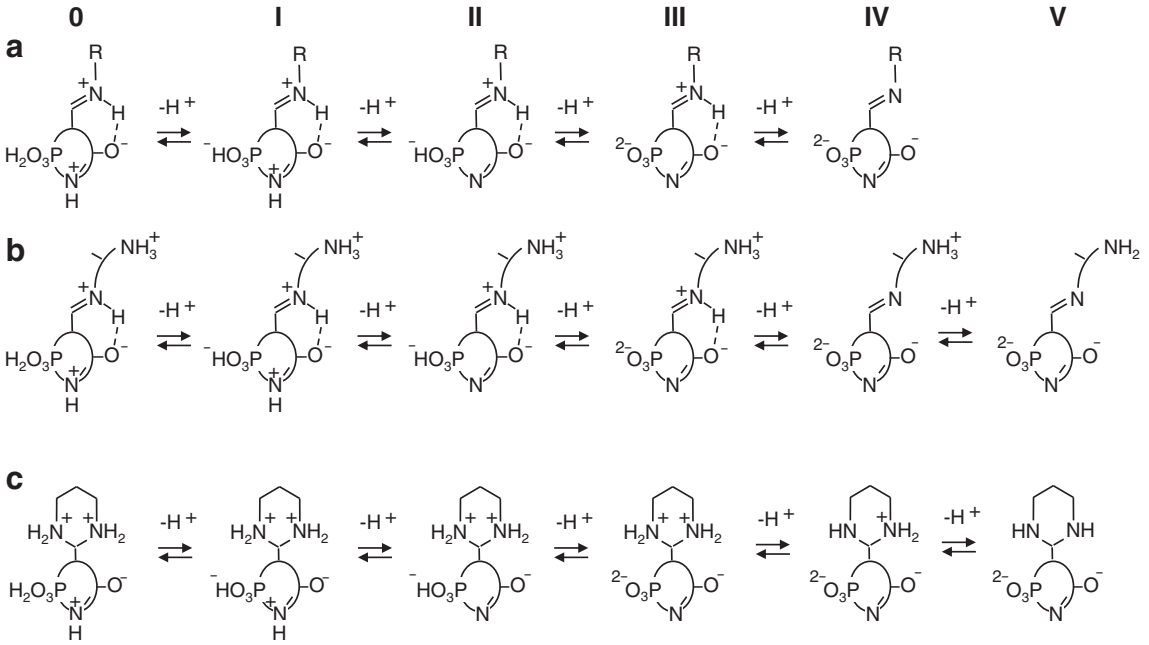

Scheme 4. Protonation states of PLP species in aqueous solution. (a) Single Schiff base, (b) Schiff base with a diamine or L-lysine, (c) geminal diamine. Adapted from Refs. [13] and [17].

In order to model more closely the biological substrates NMR studies in aqueous solution were performed of PLP in the presence of L-lysine [13]. L-lysine can form two different single headed Schiff bases with PLP, either 4 involving the α-amino group or 5, involving the ε-amino group (Fig. 2). Therefore, this system represents a model for the transimination between the internal and external aldimines of PLP. In addition, double headed Schiff bases are formed involving two molecules of PLP and one L-lysine molecule. However, as the results are not essentially different from those of the single headed ones they are not discussed further. The equilibrium between the single headed α- and ε-Schiff bases was recently studied by ^{13}C NMR of the doubly ^{13}C and singly ^{15}N labeled compounds 4 and 5 whose structure in protonation state III is depicted in Fig. 2. Information about the protonation states and the intramolecular tautomerism was obtained by ^{15}N NMR.

The pH dependence of the ^{15}N chemical shifts of the imino groups of both model systems 4 and 5 is depicted in Fig. 2. Whereas 2 exhibited only the ketoenamine form characterized by a chemical shift of 140 ppm (with respect to external solid $^{15}NH_4Cl$) in protonation state III, low-field shifts are observed for 4 and 5 indicating the presence of the enolimine form. By a quantitative analysis the equilibrium constants of tautomerism in protonation state III could be obtained, which are larger for the ε-aldimine 5 than for the α-aldimine 4. Thus, in the latter, the Schiff base nitrogen is less basic than in 2 and 5 as expected from the electronic properties of the different nitrogen substituents. When the phosphate group becomes protonated in protonation state II the equilibrium constants are somewhat smaller, in agreement with a weaker basicity of the imino nitrogen enhanced by the negative charge of the phosphate in protonation state III. However, when the pyridine N becomes protonated in state I and 0, we assume again that the ketoenamine tautomer is again entirely formed as in the methyl Schiff base 2.

An important point is that the observation of the enolimine tautomer indicates that the intramolecular OHN hydrogen bond of 4 and 5 is not broken by water molecules in aqueous solution. Even more important is that in aqueous environment, formation of the ketoenamine tautomer does not require protonation of the pyridine N.

A geminal diamine (Scheme 1d) with L-lysine which would involve a cyclic structure was not observed over the pH range studied [13]. Several other geminal diamines of PLP have been detected in solution [22,25–29]; recently, an enzymic geminal diamine formed by an internal lysine and an external glutamate could be trapped and observed by X-ray crystallography [30]. The protonation states of geminal diamines are an open question. Therefore, we have used ^{15}N NMR to study PLP in aqueous solution in the presence of doubly ^{15}N labeled diaminopropane. Here, besides the single headed Schiff base 6 and double headed Schiff base, also the cyclic diamine 7 (Scheme 5) detected previously by Metzler et al. [22] was observed and its protonation states characterized [13]. Below pH 10 both amino groups are protonated, *i.e.* protonation states 0 to III (Scheme 4c) are formed. IV is stable only in a small range around pH 11, and the deprotonated state V dominates above pH 12. It follows that, geminal diamines in natural environments usually are accompanied by a counteranion.

Fig. 3 provides an overview of the occurrence of different PLP species and their reaction partners as a function of pH. The color intensity of the vertical bars indicates schematically the probability to find a given species. The protonation states defined in Schemes 3 and 4 are represented by Roman numerals. pK_a values that have been determined are represented by horizontal lines separating the protonation states. In order to facilitate the discussion we have included schematically chemical formulas illustrating in each case the protonation state exhibiting the highest probability in the whole pH range. On the left side, the PLP species formed by reaction with diaminopropane are depicted, and on the right side those by reaction

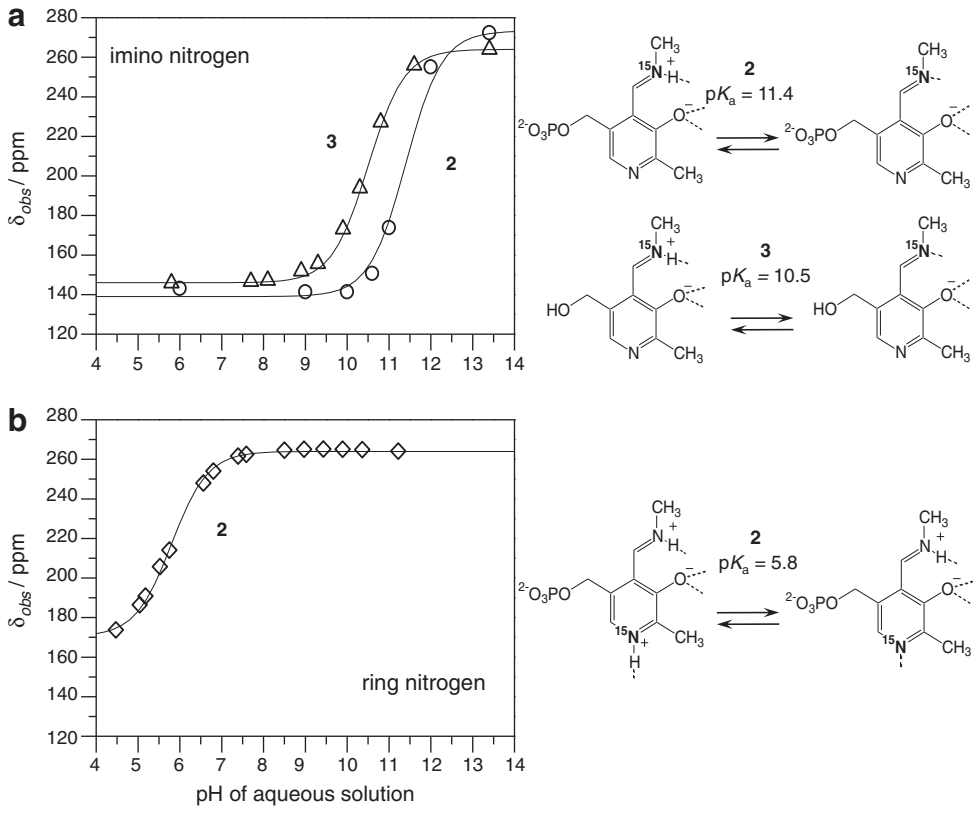

Fig. 1. ^{15}N chemical shifts of the ^{15}N-labeled Schiff bases as a function of pH. (a) ^{15}N imino labeled Schiff bases containing the side chain phosphate group (2) (symbol: open circle) and hydroxyl group (3) (symbol: open triangle). (b) ^{15}N ring labeled Schiff bases containing the side chain phosphate group (2). Adapted from Ref. [11].

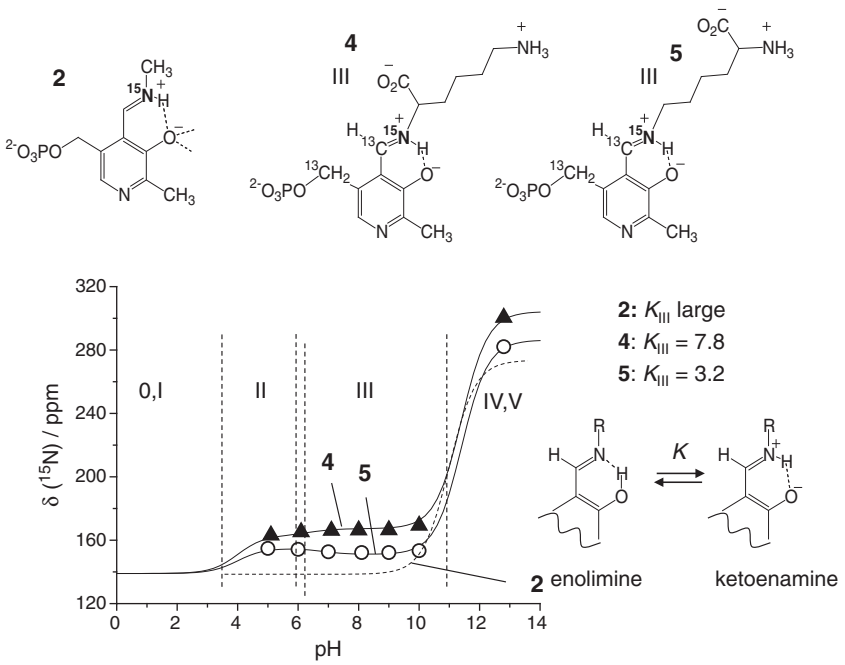

Fig. 2. Henderson–Hasselbalch plot of the ^{15}N chemical shifts of the single headed Schiff bases 4 and 5. For comparison we have added the corresponding data (dashed curve) of the PLP methylamine Schiff base (2) depicted in Fig. 1. Adapted from Ref. [13].

with L-lysine. We have omitted the results obtained for double headed Schiff bases where both amino groups of diamines or L-lysine form a Schiff base [13].

Below pH 4, only free doubly protonated L-lysine or diaminopropane is present, in a mixture with PLP for which the hydrate form 1h dominates as expected [11,12]. The formation of single headed and double headed Schiff base starts above pH 4. Whereas the single headed ε-Schiff bases 5 with PLP remains stable when pH is increased and becomes predominant at very high pH values, surprisingly, the α-Schiff base 4 hydrolyzes at pH 12 releasing free L-Lysine and PLP as aldehyde. The single headed Schiff base 6 with diaminopropane shows a particular behavior: above pH 8 it is converted into a geminal diamine species 7 which becomes the only product at very high pH.

It follows that the free energies of the different species are controlled by protonation/deprotonation processes, but how is this feature related to the acid–base properties of the individual functional groups? A look at Fig. 3 indicates that the acid–base properties of the pyridine N play the most important role. The Schiff bases loose the pyridinium proton entirely at pH 4 when protonation state I is interconverted into II; 1a and 1h loose the pyridinium proton partially, as the phenolic proton can compensate partially for this loss [11,12]. Hence, pH 4 is the starting point for the formation of the Schiff bases. They become, however, dominant only when 1h and 1a have completely lost the pyridine proton as well as the remaining phosphate proton in protonation state III. We find only minor differences in the single and the double headed Schiff bases, indicating that the two amino groups of diamines and of L-lysine can react independently of each other.

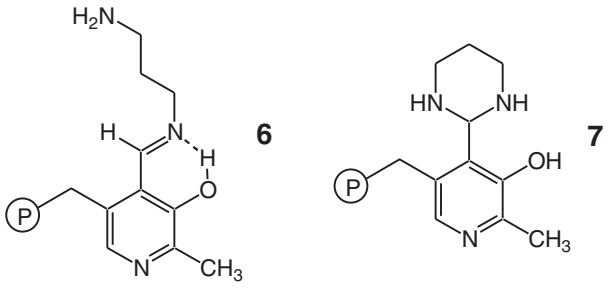

Scheme 5. Chemical structures of the single headed Schiff base of PLP with diamino propane (6) and the corresponding cyclic geminal diamine (7).

As far as the stability of the geminal diamine is concerned, it is plausible that it is destroyed by single or double protonation; double protonation could immediately have the diamine as leaving group. We note that Metzler et al. [19,21,22] had shown that other diamines do not form geminal diamines with PLP. We have tried different conditions in order to detect a geminal diamine with L-lysine at high pH; however, the double headed Schiff bases with L-lysine decompose at high pH as well as the single headed Schiff base 4 which decomposes into the aldehyde 1a and free L-lysine. Only 5 remains, entirely deprotonated in state V, but does not show any tendency to form a geminal diamine.

We conclude here with one remarkable finding: there is one pH where almost all PLP species, *i.e.* free aldehyde, hydrated PLP, and single Schiff bases are present in comparable amounts; this is around pH 7.

A second finding is important: formation of a geminal diamine requires a very basic environment. Moreover, the flexibility of a lysine side chain requires a negative entropy change for a geminal diamine to be formed.

Finally, as discussed above, Fig. 3 indicates that at physiological pH, all important PLP species, *i.e.* the aldehyde of PLP, the hydrate and the two Schiff bases of PLP with the α- and with the ε-amino group of L-lysine, representing models of the external and the internal aldimines are all almost thermodynamically equivalent. This is the consequence of a subtle balance of all acidic and basic groups, *i.e.* the phenol, pyridine N and the phosphate group, that may well have been under evolutionary pressure to be balanced.

4. Coupling of critical OHN hydrogen bonds of PLP Schiff bases in solid and liquid model environments

As hydrogen bond properties and protonation states of the internal and external aldimines of PLP in enzymes might be different than in aqueous solution we have performed NMR studies of model

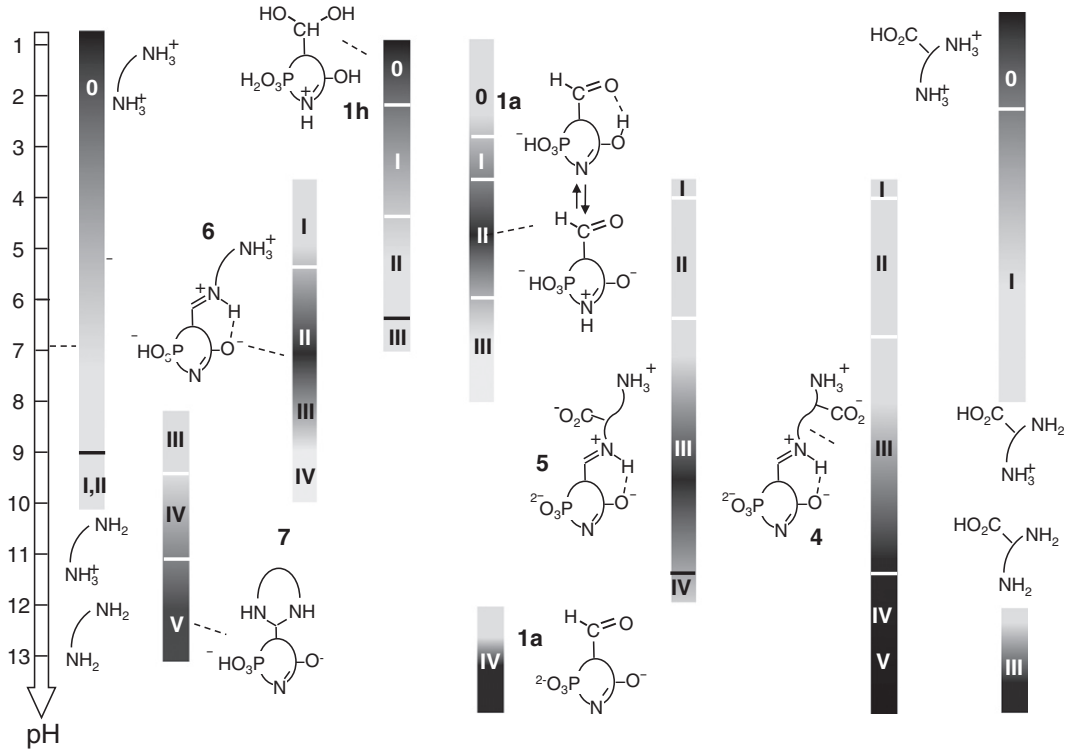

Fig. 3. Overview over pH dependent PLP species in the presence of diaminopropane (left side) and L-lysine (right side). The filled bars represent the pH range where a given species occurs, where its probability is visualized by the degree of darkness of the bar. The protonation states visualized in Scheme 3 are represented by latin numbers. Adapted from Ref. [13].

complexes in the organic solid state and in polar aprotic organic solvents. The idea was to correlate neutron crystallographic data with solid state NMR parameters, in particular chemical shifts, and then to obtain geometric information in non-crystalline environments from the NMR parameters. The results obtained are described in the following.

We start with a discussion of the geometric correlation for OHN hydrogen bonds obtained from low-temperature neutron crystallographic data. They show a correlation between the two hydrogen bond distances r_{OH} and r_{HN} of very different chemical systems [31]. The same correlation can be transformed into a correlation between the natural H-bond coordinates $q_2 = r_{OH} + r_{HN}$ and $q_1 = ½(r_{OH} - r_{HN})$ [32], depicted in Fig. 4a. For linear hydrogen bonds, the proton coordinate q_1 represents the distance between the average proton position and the hydrogen bond center and q_2 the heavy atom coordinate, which is equal to the O…N distance in the case of a linear hydrogen bond. The solid line in Fig. 4a refers to equilibrium geometries which can be calculated using *ab initio* methods. The dotted line represents a correction for anharmonic ground state vibrations. The correlation covers both the formation of the OHN hydrogen bond as well as proton transfer from O to N. When proton transfer occurs, the hydrogen bond is compressed as q_2 is decreased, but increases again after H has crossed the hydrogen bond center. The data points in the minimum come from the triclinic 4-methylpyridine–pentachlorophenol complex which exhibits the shortest known OHN hydrogen bond [33]. The great utility of the correlation is that when the distance r_{HN} is known, the distance r_{OH} can be estimated.

Distances r_{DN} of the intermolecular ODN hydrogen bonds of a number of polycrystalline complexes of 2,4,6-trimethylpyridine (collidine) [34] and of aldenamine Schiff bases [15] with carboxylic acids were obtained by dipolar ^{15}N NMR. These distances correlate well with the ^{15}N chemical shifts $\delta(O\underline{H}N)$ measured with respect to the free bases which resonate around 270 ppm with respect to external solid $^{15}NH_4Cl$. Such a correlation is depicted in Fig. 4b. When H is transferred toward N, *i.e.* the HN distance decreases, a strong high field shift of the pyridine N is observed. Thus, for a given ^{15}N chemical shift, the distance r_{HN} can be estimated, and by combination with the correlation of Fig. 4a also the distance r_{OH}.

In addition, it is well known that the chemical shift of the hydrogen bonded proton depends strongly on the distance between the heavy atoms of the hydrogen bond, resulting in a ^1H–^{15}N chemical shift correlation of the type depicted in Fig. 5. In Fig. 5a the correlation for the intermolecular OHN hydrogen bond of methyl and p-tolyl Schiff bases series 8 and 9 is depicted. Each series is constituted by the free PLP Schiff base and the corresponding 1:1 complexes with various acids, in particular carboxylic acids [17]. Both data obtained for the organic solid state as well as for polar aprotic liquids are included. The correlation represents the NMR analog of the geometric H-bond correlation of Fig. 4a. When H is shifted toward the H-bond center, it experiences a low-field shift as the O…N distance is decreased; the NH distance monotonously decreases, leading to a bell-shaped correlation curve as was found previously also for other acid–pyridine complexes [32]. A maximum proton chemical shift $\delta(O\underline{H}N)$ of about 21 ppm is expected for configurations involving the shortest O…N hydrogen bond length of about 2.45 Å predicted by the equilibrium correlation in Fig. 4a. However, only values of about 20 ppm are reached in the case of the data in Fig. 5a referring to polar liquids; values of about 19 ppm are reached in the organic solid state. This is consistent with O…N distances of slightly larger than 2.45 Å as expected for low-barrier hydrogen bonds, *i.e.* systems exhibiting a small barrier for proton transfer separating two potential wells. A similar proton tautomerism between two short H-bonds was previously observed by ^1H and ^{13}C NMR for a number of intermolecular complexes of acetic acid with pyridines [35]. Deviations from the correlation curve in Fig. 5a are also observed when H is close to oxygen, as carboxylic and alcoholic OH protons exhibit substantially different chemical shifts [36]. By contrast, since the data in Fig. 5a all refer to pyridine type compounds the chemical shifts are similar when H is close to the nitrogen of the pyridine ring. An *ab initio* calculation at the level of

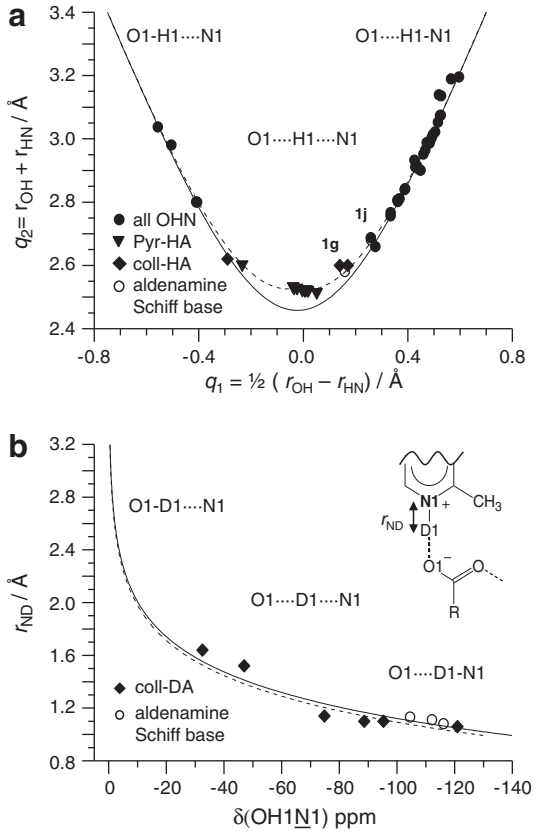

Fig. 4. Geometric OHN hydrogen bond correlations. (a) q_2 *vs.* q_1. Equilibrium (solid) and corrected (dash) correlation curves calculated according to Ref. [32] The circles refer to neutron diffraction geometries [31]. The triangles represent the recently published neutron diffraction data [33]. The diamonds correspond to crystalline 2,4,6-trimethylpyridine–acid complexes [34]. The open circles correspond to crystalline aldenamine Schiff base–acid complexes. (b) DN—distance *vs.*^{15}N chemical shift correlation. The diamonds represent the r_{HN} distances for 2,4,6-trimethylpyridine–DA complexes from dipolar solid state NMR [34] with respect to the frozen bulk 2,4,6-trimethylpyridine. The dashed line corresponds to the latter complexes calculated using a value of −130 ppm for fictive free pyridinium [32,34]. The open circles correspond to crystalline aldenamine Schiff base–acid complexes, with respect to solid 1a, resonating at 282.5 ppm. The solid line corresponds to the latter complexes by using a value of −140 ppm for fictive free pyridinium. The ^{15}N chemical shifts of the free bases are pyridine 275 ppm, collidine 268 ppm, and PLP aldenamine 282.5 ppm. Adapted from Refs. [16] and [17].

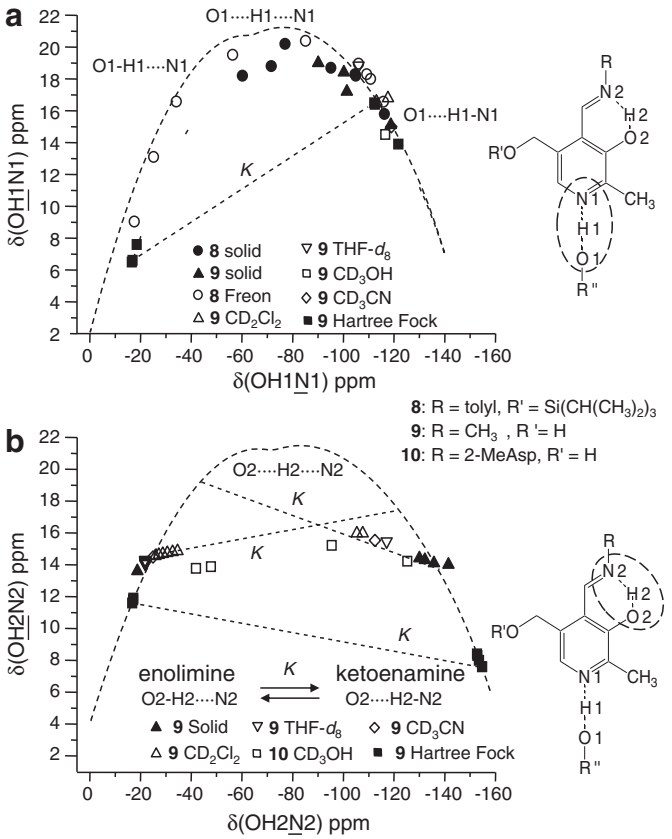

Fig. 5. ^{1}H *vs.*^{15}N chemical shift correlations. The predicted NMR parameters for the optimized geometries of the model Schiff base adducts at HF level of theory are also included. (a) Shown for the intermolecular O1H1N1 hydrogen bond for 1 and 2. The values of 1 and 2 in the organic solid state are obtained from Ref. [16]. (b) Shown for the intramolecular O2H2N2 hydrogen bond for 2 and 3. For further explanation see text. Adapted from Ref. [16].

Hartree–Fock theory reveals two tautomeric states with very different O…N distances and a large barrier separating the two states [17]. The geometries of the latter are well located on the correlation curve. A fast equilibrium between these two tautomers involving the equilibrium constant K would lead to values located on the straight dashed line in Fig. 5a. Experimentally, this is not the case. Therefore, the hydrogen bonds of carboxylic acids to the pyridine ring are strong and do not exhibit large barriers for the proton motion. It is also noteworthy that when a given complex in the organic solid state is embedded in a polar liquid such as dichloromethane or the freon mixture CDF_3/CDF_2Cl, whose dielectric constants were measured some time ago [37], the proton in the intermolecular hydrogen bond O1H1N1 is shifted strongly toward the nitrogen atom. This effect was found previously for other pyridine–acid complexes [38].

In Fig. 5b depicted is the corresponding diagram for the intramolecular OHN hydrogen bonds of 8, 9 and 10. The bell-shaped dashed ^{1}H–^{15}N correlation curve is somewhat different from the one in Fig. 5a as the imino nitrogen exhibits different chemical shifts as compared to the pyridine nitrogen. However, in contrast to the intermolecular OHN hydrogen bond, the intramolecular one does not form low-barrier hydrogen bonds as can be directly inferred from the graph. The data points are located off the correlation curve on straight lines characteristic of a fast equilibrium between the enolimine and the ketoenamine tautomers (Scheme 2). An interesting effect is observed. The dominating tautomer exhibits always a longer hydrogen bond compared to the corresponding non-dominating tautomer, as illustrated by the two dashed upper lines with opposite slope. This arises because of the polarity of the medium [39]. An increase of the dipole moment is associated in the case of the enolimine tautomer with a strengthening of the hydrogen bond and in the case of the ketoenamine tautomer with a weakening of the hydrogen bond. As the enolimine tautomer dominates in a non-polar environment, the corresponding ketoenamine exhibits then a shorter hydrogen bond as compared to a polar environment. In the latter, the ketoenamine tautomer dominates, and the corresponding enolimine exhibits a shorter hydrogen bond. We note that the computed dipole moments of the enolimine and ketoenamine species show similar trends as that described here [23].

The question now arises whether the geometries of both hydrogen bonds are coupled. For that purpose, we have depicted in Fig. 6 different correlation curves for the average proton coordinates q_1 of the two OHN hydrogen bonds. The correlation curve corresponds to series of hydrogen bond or protonation states, either arising from chemical variations, variations of the solvent polarity or of temperature.

These curves start with an initial state on the lower left side where both hydrogen bonded protons are near their respective oxygen atoms, and end on the upper right side as final state, where both protons are located on their respective nitrogen atoms. Schematically, the corresponding one-dimensional potential curves (V) are included for O1H1N1 and the free energy curves (G) for O2H2N2. Besides entropy terms, the essential difference between both types of

hydrogen bonds is the height for the barrier of proton transfer, *i.e.* small for O1H1N1 and larger for O2H2N2.

Along the correlated pathway both average proton coordinates change in the same way leading to the diagonal correlation line (i). Correlation lines (ii) and (iii) refer to uncorrelated pathways, where in (ii) first the proton in the intermolecular hydrogen bond O1H1N1 is shifted from O to N and then the proton in the intramolecular hydrogen bond O2H2N2, whereas in (iii) the contrary is realized.

A direct experimental evaluation of the pathways in Fig. 6 is difficult. For that purpose, the effects of deuteration in a neighboring hydrogen bond on the proton chemical shift of a given hydrogen bond are useful indicators, as has been shown for an intramolecular PLP model system exhibiting coupled OHO and OHN hydrogen bonds [40]. Here, in the case of PLP model Schiff bases, we obtain information about the coupling of O1H1N1 and O2H2N2 from a discussion of the corresponding ^{15}N chemical shifts, δ(O1H1N1) and δ(O2H2N2) which are both measures of the proton positions averaged over all possible tautomeric states and solvent configurations. The coupling is revealed when both values are plotted *vs.* each other as has been described previously [17] for the series of adducts 8 and 9 in the organic solid state and in polar organic solvents. The results are depicted in Fig. 7. The dashed correlation lines are presented as guides for the eye.

For solid Schiff base 8 and its solid state adducts it was found that the average OH distances of O2H2N2 are only slightly increased when H1 is shifted from O1 toward N1, a result which corresponds to pathway (ii) in Fig. 6. This finding can be associated with the low basicity of the Schiff base nitrogen carrying a tolyl group.

By contrast, the methyl Schiff base and its complexes 9 show a strong coupling of the two hydrogen bonds. When H1 is close to O1, H2 is close to O2 as found for the free base of 8 presenting an intermolecular O1H1N1 hydrogen bond with a side chain OH group of the next neighbor [14] as illustrated by the data points in Fig. 7 on the lower left side. By contrast, in the case of solid adducts with carboxylic acids where H1 is located near N1, the tautomerism in O2H2N2 favors the ketoenamine form but there is a substantial amount of the enolimine form, as illustrated by the solid triangles in Fig. 7 located near the upper dashed line. Only with the assistance of a high solvent polarity or even solvation by hydroxyl group containing solvents such as methanol, the enolimine form is suppressed, as illustrated by the data points located on the dashed diagonal line.

On the other hand, the data points for Schiff base models in aqueous solution are not located on the above mentioned curves. As was already described in Fig. 1, a ^{15}N chemical shift titration of 9 [11] indicated that above pH 11 H2 is removed from the intramolecular hydrogen bond, leading to a low-field shift to the right side on the upper dashed line in Fig. 7. At pH below 11, H2 is located in the intramolecular hydrogen bond near N2, *i.e.* only the ketoenamine tautomer is formed, independent of protonation of the pyridine N. This leads to the vertical dashed line on the left side of Fig. 7. We note again that in the case of Schiff bases with L-lysine the enolimine dominates, but that exclusive formation of the latter requires ring protonation (Fig. 2).

We draw the following conclusions. In media with dielectric constants much lower than in water, *e.g.* in polar organic solvents or in the organic solid state, the two hydrogen bonds are coupled if the basicity of the imino nitrogen and the acidity of the acid forming the intermolecular hydrogen bond to the pyridine ring are balanced as illustrated in Scheme 6a. In this case, a shift of H1 from O1 toward N1 favors the ketoenamine form. This process is assisted by local solvation by proton donors AH as illustrated in Scheme 6b. AH stabilizes the negatively charged oxygen atoms of both hydrogen bonds. In water, the stabilization of O2 is such that the pyridine N does not need any more to be protonated. However, in that case, the Schiff base does not exhibit an additional positive charge which may be required to initiate the nucleophilic attack as illustrated in Scheme 2. Also the introduction of a carboxylate group into the substituent on the imino nitrogen exhibits a similar effect [23].

5. Critical OHN hydrogen bonds of PLP in enzymic environments

In the previous sections it was shown that the hydrogen bond and protonation states of PLP Schiff bases depend on the environment, *e.g.*

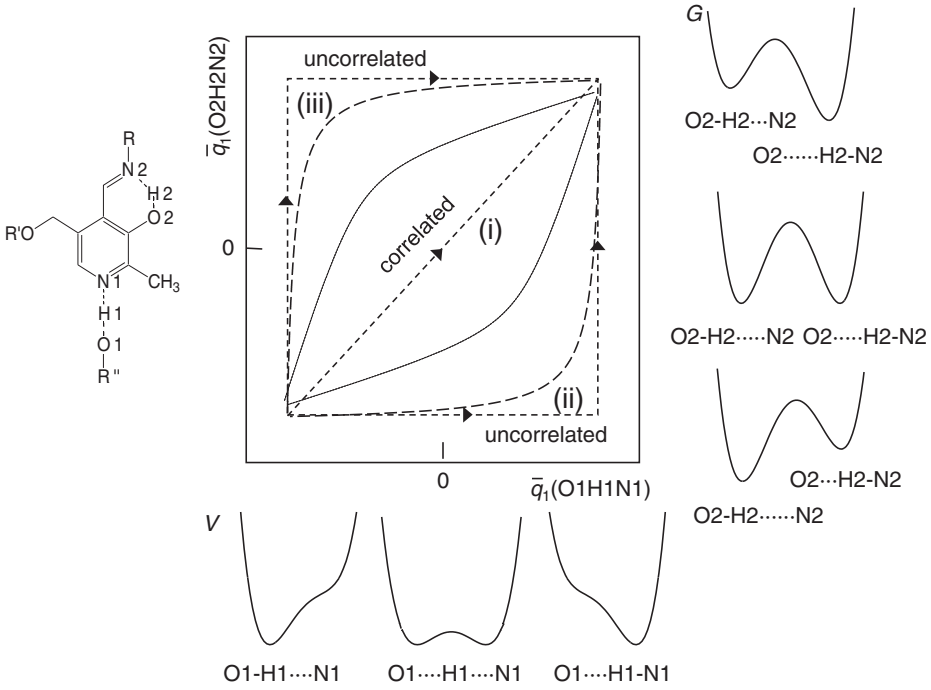

Fig. 6. Visualization of the coupling of the inter- and the intramolecular OHN-hydrogen bonds of internal and external aldimines in terms of average H-bond geometries, showing how the two average H-bond geometries may evolve in a series of stationary states, produced by changes of the structure or environments. In (i) the average geometries of both H-bonds are changed simultaneously; in (ii) the OH1N1 H-bond is first changed from the initial to the final state, and then the OH2N2 bond. In (iii) the contrary is realized. Intermediate correlation pathways are possible as indicated schematically. Adapted from Ref. [17].

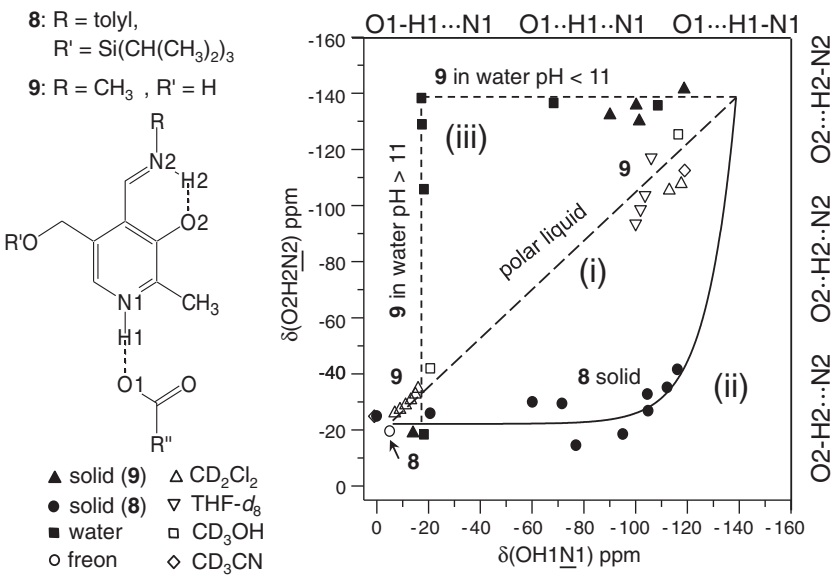

Fig. 7. Plot of the δ(O2H2N2) *vs.* δ(O1H1N1) chemical shift of 1 and 2 in different environments. The values of 8 and 9 in the organic solid state are obtained from Ref. [16]. The values of 9 in aqueous solution are obtained from Ref. [18]. For further explanation see text. Adapted from Ref. [17].

when PLP is transferred from the organic solid state to polar aprotic, protic and aqueous solution. This leads to the main question concerning PLP enzymes: which type of hydrogen bond and protonation state, *i.e.* which kind of environment is realized inside the active site. As X-ray crystallography cannot easily localize protons, and as neutron crystallography is difficult to apply to microcrystals and amorphous solids, we have recently performed liquid and solid state ^{15}N NMR experiments on the internal aldimine of PLP in *Escherichia coli* aspartate aminotransferase (AspAT, ~88 kDa), using our model studies as a reference for interpretation [18]. The ^{15}N-chemical shift–distance correlation for PLP models [14–17] reviewed in the previous section allows one to estimate the geometries of the intermolecular OHN hydrogen bonds of the pyridine ring for the different environments and to characterize the enzymic environment as described in the following.

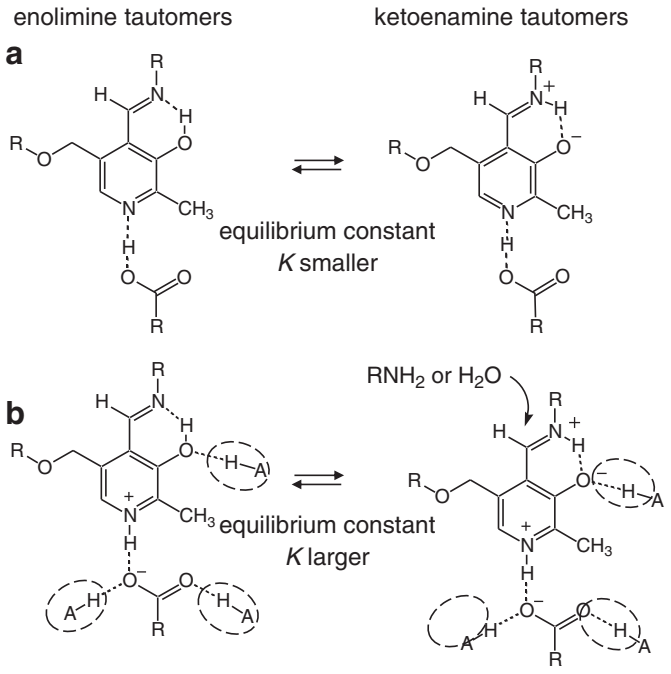

Scheme 6. Influence of ring protonation and solvation on the enolimine–ketoenamine tautomerism of PLP Schiff bases. Both phenomena favor the ketoenamine form. Adapted from Ref. [17].

In the X-ray structure of AspAT, PLP is covalently bound to Lys258 as an "internal" aldimine in the active site [41–43], where the pyridine nitrogen forms an OHN hydrogen bond to the side-chain carboxylate oxygen of Asp222 as depicted schematically in Fig. 8a. An O…N distance of 2.64 Å was observed but the position of the proton remained uncertain [42]. The distance was reported to shorten to 2.58 Å when the inhibitor maleate was bound to AspAT, which induces the closed enzyme conformation [42]. The short O…N distances could be explained in terms of a short OHN hydrogen bond. Because of the higher acidity of aspartic acid as compared to pyridinium N it was assumed that the proton is located near the pyridine N.

But is this assumption sound? According to the ^{15}N titration of Fig. 1b the pK_a of the pyridine ring of the methyl Schiff base 3 is 5.8 indicating the presence of the non-protonated ring at physiological pH. From the ^{15}N chemical shift an NH distance to hydrogen bonded water oxygen was estimated to be about 1.74 Å (Fig. 8b). The intramolecular OHN hydrogen bond is zwitterionic as discussed above. As the pK_a of the aspartic acid side chain is 4.4, a strong OHN hydrogen bond to the pyridine ring of AspAT is not plausible if the local environment is similar to that in aqueous solution, with a dielectric constant of 78.

In order to evaluate if the local environment of AspAT is like a polar aprotic environment we performed model ^{15}N NMR studies on complexes of the silylated aldenamine 8 in the presence of a protected Asp222 model, using the freon mixture $CDF_3/CDClF_2$ as solvent, which has a dielectric constant of 30 around 130 K. Both a 1:1 hydrogen bonded complex 8b (Fig. 8c) and a 2:1 complex 8c were observed. In both cases strong OHN hydrogen bonds were formed whose geometries were estimated from the ^{15}N chemical shifts [18]. In the case of 8b the proton is near oxygen, involving an H…N distance of 1.43 Å. By contrast, the proton is shifted toward nitrogen in 8c resulting in an H…N distance of 1.11 Å and an O…H distance of 1.48 Å (Fig. 8d), because the acidity of a linear acid chain is larger than of a single acid molecule [44,45].

^{15}N solid state NMR experiments were performed at 225 K on microcrystalline AspAT lyophilized at pH 6.9 [18], where the pyridine ring of PLP was specifically labeled with ^{15}N. The ^{15}N chemical shift indicated an H…N distance of 1.09 Å and an O…H distance of 1.54 Å as depicted in Fig. 8e which clearly indicates a zwitterionic structure for the intermolecular OHN hydrogen bond in AspAT. The sum of the two distances, 2.63 Å is in excellent agreement with the X-ray crystal structure, yet, NMR clearly demonstrates the presence of a proton and

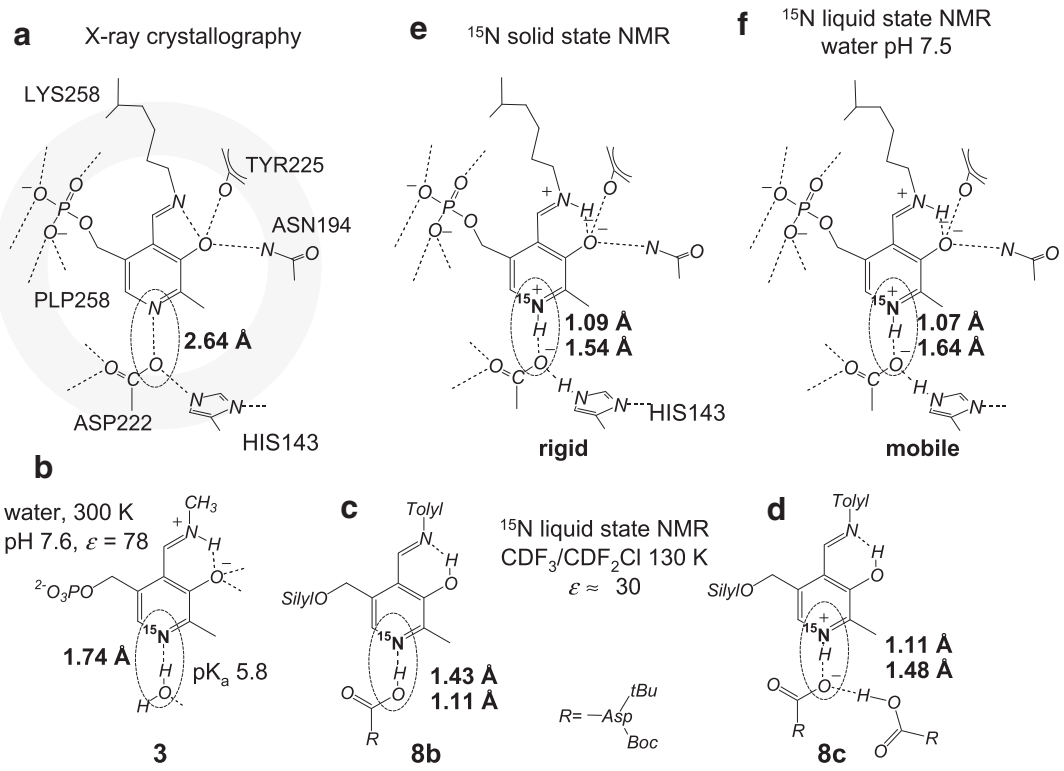

Fig. 8. Hydrogen bond geometries of holo-AspAT and related model systems. (a) X-ray crystallographic structure [43]. (b) Methyl Schiff base 3 (see Fig. 1b) in water at pH 7.6. (c) 1:1 complex 8b of the tolyl Schiff base 8 with a protected aspartic acid in CDF_3/CDF_2Cl at 130 K. (d) The analogous 2:1 complex. (e) H-bond geometry of microcrystalline holo-AspAT at 225 K studied by solid state ^{15}N NMR. (f) Corresponding geometry of holo-AspAT in aqueous solution at pH 7.5. For the values of the dielectric constant ε see Ref. [37]. For explanations see text. Adapted from Ref. [18].

provides details of its position between the N and O atoms involved in the hydrogen bond. According to the findings discussed above, the intramolecular OHN hydrogen bond must be zwitterionic, in agreement with absorption spectra of the enzyme under these conditions. For AspAT in the presence of maleate the shortening of the O…N distance observed by X-ray crystallography was confirmed by NMR [18].

A frequent question is whether the X-ray crystallographic structure is maintained in solution. This was answered for the aspartate–pyridine hydrogen bond of singly ^{15}N labeled AspAT by performing ^{15}N NMR measurements of this system in water at pH 7.5. Whereas in the solid state the ^{15}N signal is broad, due to various solid state effects including a narrow distribution of hydrogen bond geometries, a sharp ^{15}N signal was observed for the aqueous solution at pH 7.5. A small change in the signal position was observed, consistent with a slight shortening of the N…H distance and a slight increase of the H…O distance as illustrated in Fig. 8f. Thus, the zwitterionic character of the OHN hydrogen bond is somewhat increased, but the pyridine N remains protonated under physiological conditions. It follows that the pyridine N and Asp222 in the active site of the enzyme behave as in polar organic media: when they loose their water shell and come in direct contact their combined basicity leads to a high pK_a value. For the OHN hydrogen bond of the His143–Asp222 ligand of AspAT to PLP we observe a hydrogen bond geometry – both in the microcrystalline environment as well as in water – which is typical for a medium exhibiting a dielectric constant of about 30. Moreover, the pK_a values of the pyridine N and the aspartate carboxylic acid in water are not appropriate for estimating the position of the proton in the intermolecular Asp222/pyridine N OHN hydrogen bond. The enzyme must provide additional interactions to allow proton transfer to the pyridine N. The hydrogen bonds from Asp222 to His143 and two conserved water molecules in the AspAT active site are, therefore, probably the most important secondary interactions required to shorten the H…N distance and to produce active enzyme.

These results indicate that the internal aldimine of PLP in AspAT is present as a zwitterionic ketoenamine carrying an additional positive charge which activates the cofactor for nucleophilic addition (Scheme 2). This will hold for other PLP-dependent enzymes where the pyridine ring of the cofactor is involved in a hydrogen bond with a carboxylic acid group. However, in alanine racemase PLP forms an internal aldimine where the pyridine N is not protonated, rather it weakly hydrogen bonds to an arginine residue [46,47]. Thus, PLP does not appear to carry a net positive charge. Richard et al. [48] have suggested that PLP-dependent racemases sacrifice part of the cofactor's intrinsic catalytic power by using it in the neutral pyridine form. Apparently, the mechanistic imperative to direct the reaction toward proton transfer at Cα, and avoid the wasteful dead-end transamination reaction that occurs via protonation at C4′, overrides the competing imperative to utilize the cofactor in its most active form. A similar proposal was made by one of us [49]. Recently, mixed quantum/molecular mechanical simulations of this system support the presence of the ketoenamine structure induced by solvent dipoles [50,51]. This is the same situation as described in the first section for PLP Schiff bases in water above pH 6, where the ketoenamine forms dominate but where nucleophilic substitution, at least by water molecules, is slow or thermodynamically not favored. On the other hand, a positive charge might be introduced in this case by the addition of a stronger proton donor which forms a strong hydrogen bond to the phenolic oxygen or which protonates the latter as illustrated in Scheme 7. However, further studies are needed in order to understand fully the intricacies of alanine racemase.

6. Conclusions

NMR is a powerful tool to determine average hydrogen bond geometries both in the solid state and in solution. Thus, differences between both phases can be detected and the role of the polarity of

the environment on critical hydrogen bonds can be evaluated even in large proteins.

Using this method, we have shown that protonation of the pyridine ring of PLP shifts the tautomerism of the intramolecular hydrogen bond from the enolimine toward the ketoenamine form (Scheme 2). A single carboxylic group is not sufficient for protonation but needs to be assisted by a second proton donor such as histidine (Fig. 8). Full formation of the ketoenamine form requires assistance of solvation by additional proton donors. Both, the inter- and the intramolecular OHN hydrogen bonds of PLP in most PLP-dependent enzymes carry then a net positive charge as expected for the enzyme reactions to take place. However, many surrounding polar groups, in particular water, can also lead to a dominance of the ketoenamine form, without protonation of the pyridine ring. Apparently, there is then no net positive charge of PLP in alanine racemase, an unsolved problem requiring further research.

We have also shown that the OHN hydrogen bond between the aspartate residue and the pyridine N of PLP in AspAT exhibits a geometry as expected for a corresponding model system embedded in a polar organic solvent exhibiting a dielectric constant of about 30. This value is far below that of water; in the interior of a protein this local polarity is induced mostly by polar side chains and bound water molecules. Thus, the active site environment is better modeled using proton donors in polar aprotic solvents than in water.

The concept of pK_a values which describes protonation states of acids and bases in water under conditions of hydrated species breaks down in proteins where direct persistent acid–base hydrogen bonds are formed as illustrated in Fig. 9. At physiological pH, carboxylic acids AH are deprotonated in water and present as anions, and bases B of intermediate strength such as pyridine or histidine are neutral *i.e.* deprotonated in water. However, if they are brought together to interact in the interior of a protein they become very basic and may incorporate a proton from solution. The individual pK_a values of both species are replaced by an apparent pK_a value of the hydrogen bond A—H···B formed. This value corresponds to the pH in water where the bond is destroyed by removal of the proton. The location of H in the hydrogen bond cannot be predicted by the pK_a values of both groups in water. This location depends on the local electrostatics, as illustrated schematically in Fig. 9.

Whereas our conclusions refer to enzymic ground states, we note that related observations have been made for enzymic transition states of ion recombination reactions by kinetic measurements of Richard and Amyes [52] as well as by computational studies of Lluch et al. [53]. In these studies it was shown that the lower polarity inside enzymes as compared to water leads to a conversion of the solvent separated ion pairs to zwitterionic, intimate ion pair states, or in other words, to a reduction of the dipole moment of the ion pair required for the recombination reaction to occur.

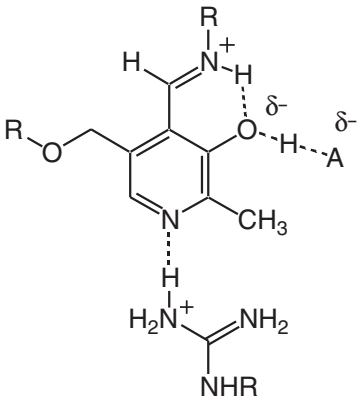

Scheme 7. Hydrogen bonding or protonation of the phenolic oxygen of PLP in alanine racemase as a possible source for a positive charge of the PLP moiety without ring protonation.

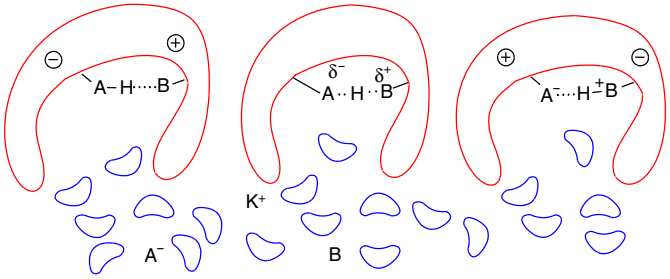

Fig. 9. Acid–base properties in water and the interior of proteins. For further discussion see text.

Acknowledgements

This work has been supported by the Deutsche Forschungsgemeinschaft, Bonn, the Fonds der Chemischen Industrie, Frankfurt, and the Russian Foundation of Basic Research.

References

[1] P. Christen, D.E. Metzler, Transaminases, 1st ed., Wiley, J. & Sons, New York, 1985, pp. 37–101.
[2] M.A. Spies, M.D. Toney, Multiple hydrogen kinetic isotope effects for enzymes catalyzing exchange with solvent: application to alanine racemase, Biochemistry 42 (2003) 5099–5107.
[3] V.N. Malashkevich, M.D. Toney, J.N. Jansonius, Crystal structure of true enzymic reaction intermediates: aspartate and glutamate ketimines in aspartate aminotransferase, Biochemistry 32 (1993) 13451–13462.
[4] X. Zhou, M.D. Toney, pH studies on the mechanism of the pyridoxal phosphate-dependent dialkylglycine decarboxylase, Biochemistry 38 (1998) 311–320.
[5] D.E. Metzler, Biochemistry, The Chemical Reactions of Living Cells, 1, Academic Press, New York, 1977, pp. 444–461.
[6] R.D. Bach, C. Canepa, Theoretical model for pyruvoyl-dependent enzymatic decarboxylation of α-amino acids, J. Am. Chem. Soc. 119 (1997) 11725–11733.
[7] E.E. Snell, S.J. Di Mari, in: P.D. Boyer (Ed.), 3rd ed., The Enzymes—Kinetics and Mechanism, 2, Academic Press, New York, 1970, pp. 335–362.
[8] E.E. Snell, W.T. Jenkins, The mechanism of the transamination reaction, J. Cell. Comp. Physiol. 54 (Supp. 1) (1959) 161–177.
[9] H.H. Limbach, G.S. Denisov, N.S. Golubev, Isotope effects in the biological and chemical sciences, in: A. Kohen, H.H. Limbach (Eds.), Hydrogen Bond Isotope Effects Studied by NMR, Taylor & Francis, Boca Raton FL, 2005, pp. 193–230, (Chapter 7).
[10] H.H. Limbach, Single and multiple hydrogen/deuterium transfer reactions in liquids and solids, in: J.T. Hynes, J. Klinman, H.H. Limbach, R.L. Schowen (Eds.), Hydrogen Transfer Reactions, 1&2, Wiley-VCH Weinheim, Germany, 2007, pp. 135–221, (Chapter 6 and references cited therein).
[11] S. Sharif, M. Chan-Huot, P.M. Tolstoy, M.D. Toney, K.H.M. Jonsson, H.H. Limbach, ^{15}N NMR studies of acid–base properties of pyridoxal 5′-phosphate aldimines in aqueous solution, J. Phys. Chem. B 111 (2007) 3869–3876.
[12] M. Chan-Huot, C. Niether, S. Sharif, P.M. Tolstoy, M.D. Toney, H.H. Limbach, NMR studies of the protonation states of pyridoxal 5′-phosphate in water, J. Mol. Struct. 976 (2010) 282–289.
[13] M. Chan-Huot, S. Sharif, P.M. Tolstoy, M.D. Toney, H.H. Limbach, NMR studies of the stability, protonation states and tautomerism of ^{13}C and ^{15}N labeled aldimines of the coenzyme pyridoxal 5′-phosphate in water, Biochemistry 49 (2010) 10818–10830.
[14] S. Sharif, D.R. Powell, D. Schagen, T. Steiner, M.D. Toney, E. Fogle, H.H. Limbach, X-ray crystallographic structures of enamine and amine Schiff bases of pyridoxal and its 1:1 hydrogen bonded complexes with benzoic acid derivatives: evidence for coupled inter- and intramolecular proton transfer, Acta Cryst. B62 (2006) 480–487.
[15] S. Sharif, D. Schagen, M.D. Toney, H.H. Limbach, Coupling of functional hydrogen bonds in pyridoxal 5′-phosphate-enzyme model systems observed by solid state NMR spectroscopy, J. Am. Chem. Soc. 129 (2007) 4440–4455.
[16] S. Sharif, G.S. Denisov, M.D. Toney, H.H. Limbach, NMR studies of solvent-assisted proton transfer in a biologically relevant Schiff base: toward a distinction of geometric and equilibrium H-bond isotope effects, J. Am. Chem. Soc. 128 (2006) 3375–3387.
[17] S. Sharif, G.S. Denisov, M.D. Toney, H.H. Limbach, NMR studies of coupled low- and high-barrier hydrogen bonds in pyridoxal 5′-phosphate model systems in polar solution, J. Am. Chem. Soc. 129 (2007) 6313–6327.
[18] S. Sharif, E. Fogle, M.D. Toney, G.S. Denisov, I.G. Shenderovich, P.M. Tolstoy, M. Chan Huot, G. Buntkowsky, H.H. Limbach, NMR localization of protons in critical enzyme H-bonds, J. Am. Chem. Soc. 129 (2007) 9558–9559.
[19] C.M. Metzler, A. Cahill, D.E. Metzler, Equilibria and absorption spectra of Schiff bases, J. Am. Chem. Soc. 102 (1980) 6075–6082.

[20] H. Christensen, Three Schiff base types formed by amino acids, peptides and proteins with pyridoxal and pyridoxal 5′-phosphate, J. Am. Chem. Soc. 80 (1958) 99–105.

[21] D.E. Metzler, Equilibria between pyridoxal and amino acids and their imines, J. Am. Chem. Soc. 79 (1957) 385–490.

[22] P.M. Robitaille, R.D. Scott, J.Y. Wang, D.E. Metzler, Schiff bases and geminal diamines derived from pyridoxal 5′-phosphate and diamines, J. Am. Chem. Soc. 111 (1989) 3034–3040.

[23] Y. Lin, J. Gao, Internal proton transfer in the external pyridoxal 5′-phosphate Schiff base in DOPA decarboxylase, Biochemistry 49 (2010) 84–94.

[24] J. Crugeiras, A. Rios, E. Riveiros, J.P. Richard, Substituent effects on electrophilic catalysis by the carbonyl group: anatomy of the rate acceleration for PLP-catalyzed deprotonation of glycine, J. Am. Chem. Soc. 133 (2011) 3173–3183.

[25] P.S. Tobias, R.G. Kallen, Kinetics and equilibria of reaction of pyridoxal 5′-phosphate with ethylenediamine to form Schiff bases, and cyclic geminal diamines—evidence for kinetically competent geminal diamine intermediates in transimination sequences, J. Am. Chem. Soc. 97 (1975) 6530–6539.

[26] R. Haran, J.P. Laurent, M. Massol, F. Nepveu-Juras, Vitamin B6, and derivatives. II—^{13}C NMR study of systems formed by pyridoxal phosphate, and pyridoxal with octopamine, Org. Magn. Res. 14 (1980) 45–48.

[27] K.G. Counts, I. Wong, M.A. Oliveira, Investigating the geminal diamine intermediate of yersinia pestis arginine decarboxylase with substrate, product, and inhibitors using single wavelength stopped-flow spectroscopy, Biochemistry 46 (2007) 379–386.

[28] R.J. Ulévitch, R.G. Kallen, Studies of reactions of substituted D,L-erythro-beta-phenylserines with lamb liver serine hydroxymethylase—effects of substituents upon de-aldolization step, Biochemistry 16 (1977) 5355–5363.

[29] M.A. Vázquez, F. Munoz, J. Donoso, Transamination reaction between pyridoxal 5′-phosphate Schiff bases with dodecylamine and amino-acids, J. Phys. Org. Chem. 5 (1992) 142–154.

[30] P.D. Cook, H.M. Holden, A structural study of GDP-4-keto-6-deoxy-D-mannose-3-dehydratase: caught in the act of geminal diamine formation, Biochemistry 46 (2007) 14215–14224.

[31] Th. Steiner, Lengthening of the covalent X—H bond in heteronuclear hydrogen bonds quantified from organic and organometallic neutron crystal structures, J. Phys. Chem. A 102 (1998) 7041–7052.

[32] H.H. Limbach, M. Pietrzak, S. Sharif, P.M. Tolstoy, I.G. Shenderovich, S.N. Smirnov, N.S. Golubev, G.S. Denisov, NMR parameters and geometries of OHN- and ODN hydrogen bonds of pyridine–acid complexes, Chem. Eur. J. 10 (2004) 5195–5204.

[33] Th. Steiner, I. Majerz, C.C. Wilson, First O—H—N hydrogen bond with a centered proton obtained by thermally induced proton migration, Angew. Chem. Int. Ed. 40 (2001) 2651–2654.

[34] P. Lorente, I.G. Shenderovich, N.S. Golubev, G.S. Denisov, G. Buntkowsky, H.H. Limbach, ^{1}H/^{15}N NMR chemical shielding, dipolar ^{15}N,^{2}H coupling and hydrogen bond geometry correlations in a novel series of hydrogen bonded acid–base complexes of collidine with carboxylic acids, Magn. Reson. Chem. 39 (2001) S18–S29.

[35] P.M. Tolstoy, J. Guo, B. Koeppe, N.S. Golubev, G.S. Denisov, S.N. Smirnov, H.H. Limbach, Geometries and tautomerism of OHN hydrogen bonds in polar solution probed by H/D isotope effects on ^{13}C NMR chemical shifts, J. Phys. Chem. A 114 (2010) 10775–10782.

[36] H.H. Limbach, P. Tolstoy, N. Pérez-Hernández, J. Guo, I.G. Shenderovich, G.S. Denisov, OHO hydrogen bond geometries and NMR chemical shifts: from equilibrium structures to geometric H/D isotope effects with applications for water, protonated water and compressed ice, Israel J. Chem. 49 (2009) 199–216.

[37] I.G. Shenderovich, A.P. Burtsev, G.S. Denisov, N.S. Golubev, H.H. Limbach, Influence of the temperature-dependent dielectric constant on the H/D isotope effects on the NMR chemical shifts and the hydrogen bond geometry of the collidine–HF complex in CDF_3/$CDClF_2$ solution, Magn. Reson. Chem. 39 (2001) S91–S99.

[38] P.M. Tolstoy, S.N. Smirnov, I.G. Shenderovich, N.S. Golubev, G.S. Denisov, H.H. Limbach, NMR studies of solid state—solvent and H/D isotope effects on hydrogen bond geometries of 1:1 complexes of collidine with carboxylic acids, J. Mol. Struct. 700 (2004) 19–27.

[39] N.S. Golubev, G.S. Denisov, S.N. Smirnov, D.N. Shchepkin, H.H. Limbach, Evidence by NMR of temperature-dependent solvent electric field effects on proton transfer and hydrogen bond geometries, Z. f. Phys. Chem. 196 (1996) 73–84.

[40] N.S. Golubev, S.N. Smirnov, P.M. Tolstoy, S. Sharif, M.D. Toney, G.S. Denisov, H.H. Limbach, Observation by NMR of the tautomerism of an intramolecular OHOHN-charge relay chain in a model Schiff base, J. Mol. Struct. 844 (2007) 319–327.

[41] J.N. Jansonius, Structure, evolution and action of vitamin B6-dependent enzymes, Curr. Opin. Struct. Biol. 8 (1998) 759–769.

[42] J. Jager, M. Moser, U. Sauder, J.N. Jansonius, Crystal structures of *Escherichia coli* aspartate aminotransferase in two conformations comparison of an unliganded open and two liganded closed forms, J. Mol. Biol. 239 (1994) 285–305.

[43] J.J. Onuffer, J.F. Kirsch, *Escherichia coli* aspartate aminotransferase by the replacement of Asp222 with alanine. Evidence for an extremely slow conformational change, Protein Eng. 7 (1994) 413–424.

[44] N.S. Golubev, S.N. Smirnov, V.A. Gindin, G.S. Denisov, H. Benedict, H.H. Limbach, Formation of charge relay chains between acetic acid and pyridine observed by low temperature NMR, J. Am. Chem. Soc. 116 (1994) 12055–12056.

[45] S.N. Smirnov, N.S. Golubev, G.S. Denisov, H. Benedict, P. Schah-Mohammedi, H.H. Limbach, Hydrogen/deuterium isotope effects on the NMR chemical shifts and geometries of intermolecular low-barrier hydrogen bonded complexes, J. Am. Chem. Soc. 118 (1996) 4094–4101.

[46] J.P. Shaw, G.A. Petsko, D. Ringe, Determination of the structure of alanine racemase from *Bacillus stearothermophilus* at 1.9 Å resolution, Biochemistry 36 (1997) 1329–1342.

[47] A.A. Morollo, G.A. Petsko, D. Ringe, Structure of a Michaelis complex analogue: propionate binds in the substrate carboxylate site of alanine racemase, Biochemistry 38 (1999) 3293–3301.

[48] J. Crugeiras, A. Rios, E. Riveiros, J.P. Richard, Substituent effects on the thermodynamic stability of imines formed from glycine and aromatic aldehydes: implications for the catalytic activity of pyridoxal-5′-phosphate, J. Am. Chem. Soc. 131 (2009) 15815–15824.

[49] M.A. Spies, J.J. Woodward, M.R. Watnik, M.D. Toney, Alanine racemase free energy profiles from global analyses of progress curves, J. Am. Chem. Soc. 126 (2004) 7464–7475.

[50] D.T. Major, J. Gao, A combined quantum mechanical and molecular mechanical study of the reaction mechanism and α-amino acidity in alanine racemase, J. Am. Chem. Soc. 128 (2006) 16345–16357.

[51] A. Rubinstein, D.T. Major, Understanding catalytic specificity in alanine racemase from quantum mechanical and molecular mechanical simulations of the arginine 219 mutant, Biochemistry 49 (2010) 3957–3964.

[52] J.P. Richard, T.L. Amyes, On the importance of being zwitterionic: enzymatic catalysis of decarboxylation and deprotonation of cationic carbon, Bioorg. Chem. 32 (2004) 354–366.

[53] E. Puig, M. Garcia-Viloca, A. González-Lafont, J.M. Lluch, On the ionization state of the substrate in the active site of glutamate racemase. A QM/MM study about the importance of being zwitterionic, J. Phys. Chem. A 110 (2006) 717–725.